# Magnetization and resistivity of $UNi_4B$ in high magnetic fields

S.A.M. Mentink* and G.J. Nieuwenhuys
*Kamerlingh Onnes Laboratory, Leiden University, P.O. Box 9506, 2300 RA Leiden, The Netherlands*

H. Nakotte†
*Van der Waals–Zeeman Laboratory, University of Amsterdam, Valckenierstraat 65, 1018 XE Amsterdam, The Netherlands*

A.A. Menovsky
*Kamerlingh Onnes Laboratory, Leiden University, P.O. Box 9506, 2300 RA Leiden, The Netherlands*
*and Van der Waals–Zeeman Laboratory, University of Amsterdam, Valckenierstraat 65, 1018 XE Amsterdam, The Netherlands*

A. Drost and E. Frikkee
*Netherlands Energy Research Foundation ECN, P.O. Box 1, 1755 ZG Petten, The Netherlands*

J.A. Mydosh
*Kamerlingh Onnes Laboratory, Leiden University, P.O. Box 9506, 2300 RA Leiden, The Netherlands*
(Received 16 November 1994)

The hexagonal uranium intermetallic compound $UNi_4B$ orders antiferromagnetically below $T_N = 20$ K in a magnetic structure, where, in zero applied magnetic field, one-third of the spins remains paramagnetic. Here, we report on the high-field ($B \leq 50$ T) magnetic and transport properties of this material. We establish the magnetic structures and phase diagram and the influence of magnetic field on the paramagnetic spins. Model calculations of the magnetization assuming two independent spin systems are in qualitative agreement with the observed magnetization.

## I. INTRODUCTION

In previous papers[1–3] we have presented the magnetic structure and low-temperature magnetic behavior of the hexagonal intermetallic compound $UNi_4B$, crystallizing in a superstructure of the $CeCo_4B$-type structure. The geometrical frustration that inhibits antiferromagnetic order in a triangular lattice is partially lifted by the formation of a crystallographic superstructure. In the enlarged unit cell the uranium atoms are located at positions with different site symmetries, i.e., with different configurations of their neighboring nickel atoms. The details of this unusual superstructure, which is investigated by single-crystal x-ray and neutron diffraction, will be reported elsewhere.[4] Here it suffices to mention that in a first approximation the superstructure is related to the $CeCo_4B$ subcell by a rotation over 30° in the basal plane, combined with an elongation of $a_{sub}$ by a factor $\sqrt{3}$, yielding superstructure-lattice parameters $a' = \sqrt{3}a_{sub}$ and $c' = c_{sub}$.

Below $T_N = 21(1)$ K magnetic intensity is found at distances $\pm\vec{Q} = (\frac{1}{3}\ \frac{1}{3}\ 0)_{super}$ from the reciprocal lattice points of the superstructure.[1] This $\vec{Q}$ vector describes the hexagonal magnetic unit cell with axes parallel to those of the subcell, and $a_{magn} = 3a_{sub}$. The absence of magnetic $(h\,k\,1)$ and the presence of magnetic $(h\,k\,2)$ reflections give $c_{magn} = \frac{1}{2}c_{sub}$; i.e., the order is ferromagnetic along the $c$ axis. In terms of the reciprocal lattice of the $CeCo_4B$ subcell, the ordering wave vector is $\vec{Q} = (0\ \frac{1}{3}\ 0)_{sub}$. The unique antiferromagnetic spin arrangement in the $ab$ plane, realized in $UNi_4B$, is displayed in Fig. 1. Only two-thirds of the moments (with mag-

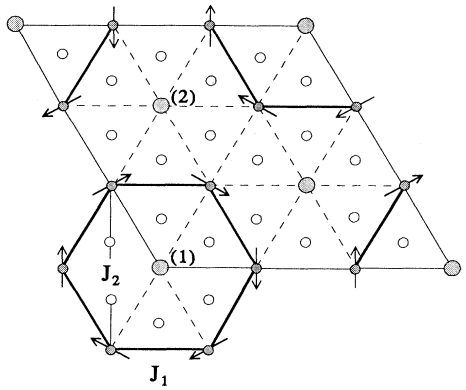


FIG. 1. Zero-field magnetic structure of hexagonal $UNi_4B$, projected on to the basal plane. The magnetic layers are stacked ferromagnetically along the $c$ direction. The thin solid lines represent the magnetic unit cell. The solid circles, labeled (1) and (2), represent the paramagnetic uranium moments, located in between the hexagonally ordered ones. The nearest- and next-nearest-neighbor magnetic coupling constants are indicated by $J_1$ and $J_2$.

0163-1829/95/51(17)/11567(7)/$06.00

nitude $1.2\mu_B$ per uranium atom) are ordered, forming a vortexlike arrangement with 60° angles between adjacent spins. The remaining one-third of the spins stays paramagnetic. This ordering pattern corresponds to the magnetic space group $P6/m'mm$, Shubnikov group 235/191 (see, e.g., Ref. 5). The sixfold and threefold rotation axes from the symmetry elements actually imply that the magnetic moments at the positions (1) and (2) in Fig. 1 cannot be ordered antiferromagnetically.

The coexistence of ordered and disordered spins manifests itself in the low-field susceptibility $\chi(T)$ by a cusp at $T_N = 20\,\mathrm{K}$, followed by an increase of $\chi$ when the temperature decreases below around 16 K.[1] Recent susceptibility data show that the paramagnetic uranium moments, surprisingly, do not undergo a phase transition down to millikelvin temperatures.[6] Also, the neutron-diffraction intensities of the $(\frac{1}{3}\,\frac{1}{3}\,0)$ and $(\frac{4}{3}\,\frac{4}{3}\,0)$ reflections, which are related to the disordered spins, do not change with temperature from 30 K (above $T_N$) to 2 K, and the intensities of the reflections belonging to the ordered moments, such as the $(\frac{2}{3}\,0\,0)$ and $(\frac{1}{3}\,0\,2)$ reflections, do exhibit a regular increase below $T_N$ without sudden changes of slope at lower $T$. Furthermore, the internal field as measured by muon spin resonance ($\mu$SR) shows a similar regular temperature dependence.[7] The magnetic planes are coupled ferromagnetically (FM) along the $c$ axis. For the paramagnetic moments stacked along the $c$ axis, this interaction is proposed to create one-dimensional (1D) spin chains with FM correlations that exist within the ordered spin matrix and behave independent of it. The anomalous excitations observed below $T_N$ then originate mainly from those inside these chains.

In this paper, we apply large pulsed magnetic fields up to 50 T and study their effects along the various high-symmetry axes of $UNi_4B$. Both magnetization, Sec. II, and electrical resistivity, Sec. III, have marked field dependences, in which the division of the spin system into two separate subsystems becomes evident. We explain the strong magnetic anisotropy using an $XY$ model with weak intraplane and strong interplane exchange coupling. We present a model calculation on a small two-dimensional lattice of $XY$ spins to obtain the magnetization and phase diagram. The results are shown to be in qualitative agreement with experiment. Finally, the magnetic phase diagram is presented and discussed in Sec. IV.

## II. MAGNETIZATION IN HIGH MAGNETIC FIELDS

The measurements presented below were performed on two different, unannealed, single crystals of $UNi_4B$. The magnetization and most of the magnetoresistivity data were taken on a Czochralski-grown crystal using natural boron, while part of the magnetorestivity was measured on the crystal with enriched $^{11}B$, earlier used to determine the magnetic structure via neutron scattering. The subcell lattice parameters of these two crystals were identical, $a = 4.953$ Å and $c = 6.964$ Å. Annealing of $UNi_4B$ up to 800 °C did not change the physical properties. The high-field magnetization experiments up to 35 T were performed at the pulsed-field facility at the University of Amsterdam, and additional data up to 52 T were taken at Osaka University.[8] The field pulses at Amsterdam have a controlled shape, with a duration up to 1 sec. The higher fields at Osaka involve less controlled pulses, with a total duration of 0.1 sec. Data were taken at $T = 1.4$ and 4.2 K. Magnetization isotherms in fields up to 12 T have been measured at Leiden University using a vibrating sample magnetometer from 1.4 to 30 K. The field was aligned parallel to the $c$ axis and for two in-plane directions, $a$ and $b$, with the $b$ axis defined perpendicular to $a$.

Figure 2 displays high-field magnetization data taken at 1.4 and 4.2 K with fields along $a$ and $c$ [see Fig. 2(a)] and the $b$ axis [see Fig. 2(b)]. Note the large anisotropy between the easy plane and hard $c$-axis magnetization, $M_{\mathrm{plane}}/M_c \approx 10$ for fields below 25 T. Along the $c$ axis, the magnetization is completely linear with field and reaches $0.12\mu_B$/f.u. at 35 T.[2] In low fields, for both in-plane directions, the magnetization is not linear, but slightly S shaped, suggesting rapid alignment of the free spin chains by applied fields of a few T. Also, the increase of the magnetization versus temperature below $T_N$ is significantly reduced by such fields.[1,2] In large fields above 7 T, small steps in the magnetization of order $0.05\mu_B$/U atom occur, with significant in-plane anisotropy. If the field is applied along $a$, three hysteretic "metamagnetic" phase transitions are observed. The

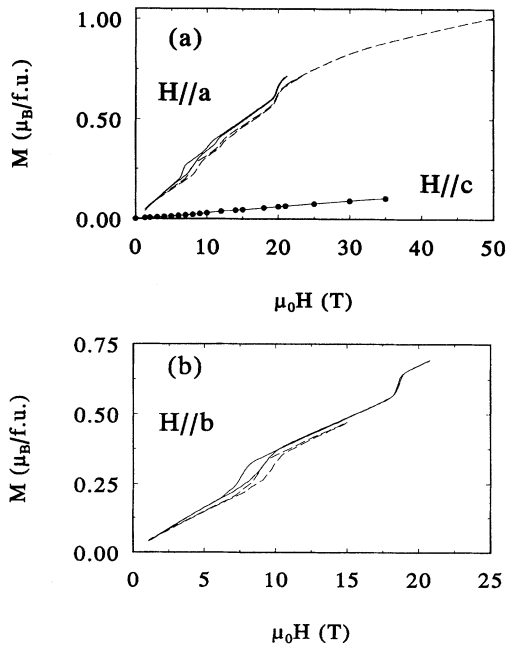


FIG. 2. High-field magnetization of $UNi_4B$ (a) with field parallel to the $a$ axis at $T = 1.4$ K (solid line) and 4.2 K (dashed line) and parallel to the $c$ axis at 4.2 K (•); (b) with field parallel to the $b$ axis (perpendicular to $a$ in the basal plane) at 1.4 K (solid line) and 4.2 K (dashed line).

transition fields are labeled $\mu_0 H_2 = 8.2$ T, $\mu_0 H_3 = 11.7$ T, and $\mu_0 H_0 = 19.8$ T. We will also use $B_i$ (with $i = 0,1,2,3$, to refer to these transition fields). At 1.4 K the respective values are 7.0, 10.8, and 19.8 T. Along $b$ only two transitions occur; the first transition field is $\mu_0 H_1 = 9.3$ T at 4.2 K. The two fields at 1.4 K are $\mu_0 H_1 = 8.1$ T and $\mu_0 H_0 = 18.6$ T. We have not measured through the higher transition at 4.2 K. The small magnetization jumps exlude first-order spin-flip processes, where spins directly flip over in the field direction. Such transitions would involve jumps of large fractions of the ordered moment of $1.2\mu_B$. None of the standard terms, spin-flop, spin-flip, or metamagnetic transition, apply to our observations in their original meaning, and from now on we refer to them as "reorientation" fields and transitions. Interestingly, the in-plane magnetizations still do not saturate in fields as large as 52 T.[8] This implies antiferromagnetic nearest-neighbor (NN) and next-nearest-neighbor (NNN) coupling between the U moments. The value of $1.2\mu_B$ per U moment is exactly recovered, if the magnetization per formula unit is extrapolated in a plot of $M$ vs $1/H$ towards $1/H = 0$ (not shown), indicating that the paramagnetic spin also reaches $1.2\mu_B$ in high fields. The value of the paramagnetic spin in zero field is not known, and difficult to estimate from the low-field susceptibility due to the rapid saturation at low temperatures.[1]

In a first approximation, the large anisotropy between $c$-axis and in-plane magnetization can be understood within a quasi-one-dimensional $XY$ model with strong interplane coupling $J$ (along the chains, parallel to the $c$ axis, ferromagnetic) and weak intraplane coupling $J'$ (between chains in the $ab$ plane, antiferromagnetic).[9,10] In such a mean-field model, the 3D ordering temperature is largely induced by the finite correlation length $\xi$ within the individual chains, irrespective of the sign of $J$:[10]

$$|J'|S^2\xi(T_N) = C_n k_B T_N, \tag{1}$$

with $C_n$ a constant depending on the spin dimensionality ($n = 2$ for $UNi_4B$). Equation (1) can be simplified[11] and expressed in terms of the ordering temperature $T_N$ and the number of neighboring chains, $z$:

$$2zJ' = k_B T_N. \tag{2}$$

With $z = 6$ for $UNi_4B$, $J'/k_B$ is estimated to be $-1.7$ K (negative for antiferromagnetic coupling). We identify $J'$ with the in-plane next-nearest-neighbor interaction, since it is this interaction which is most important in stabilizing the zero-field structure. The axial or interplane exchange constant $J$ may be derived from our analysis[1] of the low-temperature specific heat using the Bonner-Fisher results for the one-dimensional FM chain.[12] We have found $J/k_B = 35$ K. Note that the high-temperature susceptibility does not yield a positive Curie-Weiss temperature. We attribute this to the effects of crystal-field interactions, which are dominant in this temperature range. Accordingly the anisotropy of the exchange parameters is estimated to be

$$J/J' = 21, \tag{3}$$

which corresponds reasonably well to the experimentally observed anisotropy in the magnetization of 11.5 at low fields, decreasing to about 10 in the field range from 7 to 25 T.

Up until now, only the magnetic structure in zero applied field has been determined. We have performed a model calculation of the magnetization, in order to gain more insight into the nature of the spin-reorientation phases and the small magnetization steps observed in the spin-reorientation transitions. For simplicity we assume that the spins are free to rotate in the plane and that the paramagnetic spins are absent. The latter assumption is not likely to seriously affect the results in low fields, even though the moments may be substantial, but in high fields the two different moments (ordered and paramagnetic) will no longer form two separate subsystems. Therefore, we have concentrated on the low-field region for the choice of the parameters.

The magnetization $M = \partial E_0/\partial H$ follows after minimization of the energy (at $T = 0$) $E_0$ of the spin Hamiltonian

$$\mathcal{H}_{\text{magn}} = J_1 \sum_{\text{NN}} S_i S_j + J_2 \sum_{\text{NNN}} S_i S_j + \sum_{\text{spins}} K_6 \sin(6\phi) + g\mu_B \sum_i S_i \vec{H}. \tag{4}$$

This Hamiltonian acts on a $6\times6$ hexagonal plane of classical spins ordered in the zero-field magnetic structure. NN and NNN have their usual nearest-neighbor and next-nearest-neighbor meaning, with $J_1$ the NN interaction (along the crystallographic $a$ direction), and $J_2$ the NNN interaction (along the perpendicular $b$ direction). See Fig. 1. The Hamiltonian of Eq. (4) only considers the $x$ and $y$ components of the uranium spins. $K_6$ determines the in-plane anisotropy, and $\phi$ is the angle of the spins with the positive $x$ axis. The resulting magnetization is divided by 36, thus obtaining the magnetization per U atom. Any additional (unknown) contribution from the paramagnetic moments increases the total magnetization.

Via the minimalization procedure, the parameters

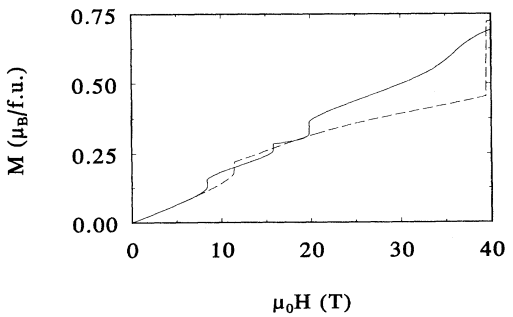


FIG. 3. Calculated magnetization isotherm of $UNi_4B$, with fields parallel to the $a$ (solid line) and $b$ (dashed line) axes, assuming $XY$ spins and the Hamiltonian given by Eq. (4).

TABLE I. Measured and calculated spin-reorientation transition fields and magnetization steps for $UNi_4B$ with fields parallel to the $a$ and $b$ directions, with temperature $T = 4.2$ K.

| | $H\|\|a$ | | | | $H\|\|b$ | | | |
|---|---|---|---|---|---|---|---|---|
| $B_{SF}$ | $B_{meas}$ (T) | $B_{calc}$ (T) | $\Delta B_{meas}$ ($\mu_B$/U) | $\Delta B_{calc}$ ($\mu_B$/U) | $B_{meas}$ (T) | $B_{calc}$ (T) | $\Delta B_{meas}$ ($\mu_B$/U) | $\Delta B_{calc}$ ($\mu_B$/U) |
| $B_1$ | | | | | 9.3 | 11.5 | 0.078 | 0.041 |
| $B_2$ | 8.2 | 8.4 | 0.043 | 0.031 | | | | |
| $B_3$ | 12.1 | 15.8 | 0.030 | 0.026 | | | | |
| $B_0$ | 19.8 | 19.8 | 0.053 | 0.046 | 18.6[a] | 39.5 | 0.066[a] | 0.27 |

[a]Value at $T = 1.4$ K .

which best describe the lowest spin-reorientation fields and steps with fields along the $a$ and $b$ directions are $J_1 = 0$, $J_2/k_B = -1.75$ K and $K_6/k_B = 0.15$ K (equal to 0.23 T). Note that the calculated value of $J_2/k_B$ is very close to the $-1.7$ K we have estimated in the $XY$ model by the number of neighbors and the Néel temperature. The calculated magnetization for fields applied along the $a$ and $b$ axes is displayed in Fig. 3, and the calculated and experimental spin-reorientation fields and magnetization steps are collected in Table I. We illustrate the proposed spin rotations in Fig. 4, where the calculated magnetic structures after the first transitions are presented, for both field parallel to the $a$ ($B = 8.8\,\mathrm{T} > B_2$) and $b$ ($B = 12\,\mathrm{T} > B_1$) axes. When compared with the zero-field structure of Fig. 1, one notices that the spins have only very gradually turned towards the field direction. The 180° angles of different pairs of spins with fields parallel to $b$ explain the sharp spin-flip-type highest transition at $B_0$, whereas the smaller angles for fields parallel to $a$ only yield small magnetization steps. Both jump field and step height agree nicely with experiment, especially at the lower transitions. This emphasizes the crucial importance of the next-nearest-neighbor interactions $J_2$ in $UNi_4B$, which was already suggested by the absence of $J_1$, and the in-plane anisotropy.

The calculated overall magnetization is too small, but it becomes very close to the observed values if a paramagnetic contribution from the free moments is incorporated. Therefore, as proposed before, for zero-field properties,[1] also in appreciable magnetic fields the spin system can be described by two rather independent subsystems. In the calculations, the magnetization reaches saturation in fields close to 40 T, occurring gradually for fields along $a$ and with a sudden final step for fields along $b$ at 39.5 T. If we assume that the paramagnetic moments have also attained $1.2\mu_B$, the calculated magnetization in 40 T is $1.05\mu_B$/f.u., in good agreement with the observed value of $1.0\mu_B$/f.u. Discrepancies that remain with our simple model are the very high value of the second spin-reorientation transition for fields along the $b$ axis and the rather large $B_3$ for fields parallel to $a$.

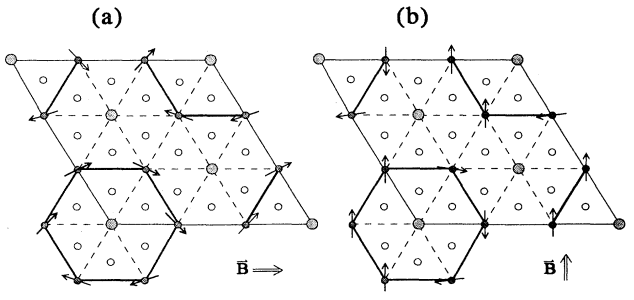


FIG. 4. Calculated spin structures of $UNi_4B$ after the first reorientation field (a) with $B = 8.8\,\mathrm{T} \,||\, a$ and (b) with $B = 12\,\mathrm{T} \,||\, b$. Note the small rotations of the spins compared to the zero-field structure of Fig. 1, explaining the small magnetization steps.

## III. ELECTRICAL TRANSPORT IN MAGNETIC FIELDS

A huge anisotropy of $UNi_4B$ in transport properties has been resolved by resistivity and thermoelectric power measurements.[1,13] In the easy plane, the resistivity is 3 times larger than along the hard $c$ axis. $T_N$ is only prominently visible for currents flowing in the $c$ direction, where a sharp drop in $\rho(T)$ signals the long-range magnetic order with its ferromagnetic coupling along $c$. For currents in the basal plane, $T_N$ is reflected by a small increase of the resistivity, indicating the formation of magnetic superzone boundaries. Below we will show the large effects in the resistance along both directions, when a large magnetic field is applied in the ordered state. The modeling of the magnetization in terms of two separated spin systems suggests a similar separation in the high-field magnetoresistance. We have measured the longitudinal and transversal magnetoresistance on the single crystals used for the above magnetization and neutron-diffraction[1] experiments.

Figure 5 displays the transversal magnetoresistance $\Delta\rho$ of $UNi_4B$, with $H \,||\, a$, $i \,||\, c$, in fields below 7 T at temperatures from 1.4 to 6 K. $\Delta\rho$ initially increases with field, until a maximum is reached around 2.8 T for $T = 1.5$ K. The field of the maximum decreases with increasing temperature, falling to zero for temperatures above $T = 7$ K. In this field range a spin-reorientation transition has not yet occurred, so that the maximum in $\Delta\rho$ may originate from the saturation of the scattering by the paramagnetic chains. Note that this field scale is the same, but more prominently visible as that which governs the low-field, low-temperature susceptibility and magnetization anomalies, described in Sec. II. The maximum certainly

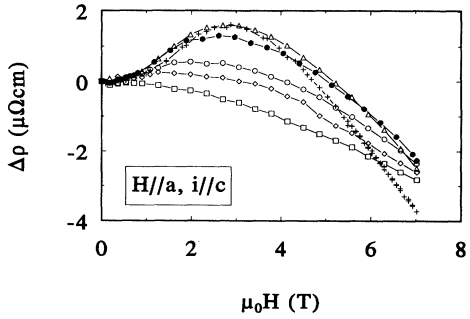


FIG. 5. Transversal magnetoresistance ($H \parallel a$, $i \parallel c$) for $UNi_4B$ with fields up to 7 T at temperatures $T = 1.5$ (+), 2.0 (△), 2.5 (•), 3.5 (○), 4.5 (◇), and 6.0 K (□). Note the maximum in $\Delta\rho$, which shifts to lower fields as the temperature increases.

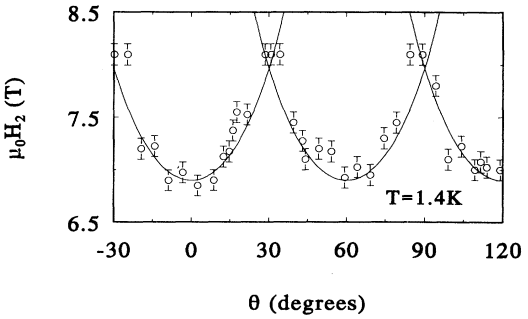


FIG. 7. Angular dependence of the first spin-reorientation field $B_2$ derived from magnetoresistance data at $T = 1.4$ K. The angle is defined in degrees from the $a$ axis. The solid line describes the $(1/\cos\theta)$ behavior of $B_2$. The error in angle is less than 2°.

signals a crossover from a low-field state, in which the magnetic field increases the scattering, to a state where the spin disorder is progressively quenched by the field. The proposed alignment of the free spin chains by fields of order 3 T is consistent with this conjecture.

The difference in this low-field region for currents applied either in the plane or parallel to the $c$ axis shows up dramatically as an inverse effect in $\Delta\rho$. Figure 6 shows the magnetoresistance at 1.5 K for fields up to 12 T parallel to $b$, with currents along $b$ and $c$, respectively. With $i \| b$, $\Delta\rho$ immediately *decreases* with increasing field, opposite to the effect described above for currents parallel to the $c$ axis. The absolute value of $\Delta\rho$ for $i \| b$ is of the same order as that for $i \| c$ for low fields. Also note the completely field-independent longitudinal magnetoresistance when both field and current are directed along the $c$ axis. This again reflects the large planar anisotropy of $UNi_4B$. The first spin-reorientation transition is evident as the sharp, field-hysteretic, drop of $\Delta\rho$. From Fig. 6 we deduce $B_1 = 8.2$ T, in agreement with the 8.1 T obtained from the magnetization experiments at this temperature. Here the anisotropy with respect to the *current* direction

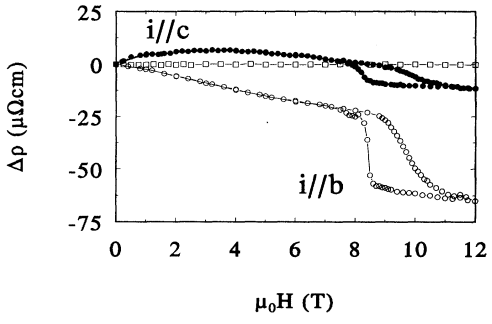


FIG. 6. Magnetoresistance of $UNi_4B$ at $T = 1.5$ K with current $i \| c$ and field $H \| b$ (•) and $i, H \| b$ (○). Data for both current and field parallel to the hard $c$ axis, taken at $T = 4.2$ K, are indicated by □.

is manifested by the 4 times larger absolute value of the resistivity jump for $i \| b$ compared to $i \| c$.

The anisotropy of the first spin-reorientation field is demonstrated in a transversal magnetoresistance experiment, at $T = 1.4$ K, with the current along the $c$ axis and field parallel to a direction rotating over 150° in the plane between the various $a$ and $b$ axes. Figure 7 displays the angular dependence of the spin-reorientation field $B_2 = \mu_0 H_2$, equaling 7.0 T for fields parallel to $a$ at 1.5 K (again in accordance with the magnetization data). Along $b$ this transition field was defined as $B_1 = \mu_0 H_1$ and equals 8.1 T. $B_2$ is seen to closely follow a $(1/\cos\theta)$ behavior, which is expected from a regular field projection onto the easy axis, with $\theta$ the angle between the $a$ axis and the magnetic field.

## IV. MAGNETIC PHASE DIAGRAM AND DISCUSSION

In Secs. II and III the main field transitions of antiferromagnetic $UNi_4B$ have been presented. The small magnetization steps suggest that these transitions involve only slight alterations of the zero-field magnetic structure. The role of the paramagnetic moments in the field range up to 50 T in determining the various spin structures is unknown, but we may speculate that they are rather unimportant. If these moments would order together with those of the known ordered structure, a largely different magnetic structure is expected. This, in turn, would lead to larger magnetization and resistance anomalies than those observed. In-field neutron-diffraction experiments are necessary to resolve this important question. However, it is shown that a separation into two magnetic subsystems, one following the calculated magnetization and the other tracking paramagnetic behavior, gives a reasonable description of the experimental results.

Combination of all magnetization, magnetoresistivity, and specific-heat[2] data yields the magnetic phase diagram of $UNi_4B$, with fields parallel to both the $a$ and $b$ axes, displayed in Fig. 8. Since no further magneti-

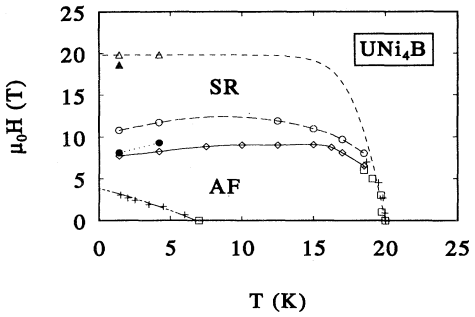


FIG. 8. Magnetic phase diagram of $UNi_4B$ for fields parallel to the basal-plane axes $a$ (open symbols) and $b$ (solid symbols) as derived from magnetoresistance (+), specific-heat (□), and magnetization (other symbols) experiments. The dot-dashed line at low fields marks the crossover line (see text). AF denotes the antiferromagnetic and SR the spin-reorientation phases.

zation steps have been observed up to 52 T, the transition field ($B_0$) of 19.8 T ($\| a$, open symbols) and 18.6 T ($\| b$, solid symbols) is taken as the magnetically ordered to paramagnetic phase boundary. The various spin-reorientation fields at different temperatures divide the spin-reorientation phases. The low-temperature, low-field region is indicated by a dot-dashed line. This crossover line denotes the maxima as observed in the magnetoresistance measurements. We propose that for fields above this crossover line, the fluctuations in the 1D-FM chains are effectively quenched. This should be confirmed by specific-heat experiments in high magnetic fields below 1 K, as above 2 K the specific heat is relatively unaffected by fields up to 6 T.[2] It is noted that phase diagrams of stacked *triangular* magnetic lattices with similar antiferromagnetic intraplane and ferromagnetic interplane interactions have recently been calculated by Plumer *et al.* using Monte Carlo simulations.[14] Although the appearance of the phase diagram of $UNi_4B$ is similar to that of triangular lattices, the hexagonal ordering of $UNi_4B$ and its in-plane anisotropy prevent a direct comparison with this theoretical work.

In conclusion, the special magnetic properties of $UNi_4B$ can be understood in a highly anisotropic $XY$ spin model, with exchange constants $J_{\|c} \simeq 20 J_{\perp c}$. The uranium moments align in the basal plane, perpendicular to the direction of the strongest hybridization. The unusual zero-field magnetic structure is stabilized by the dominant next-nearest-neighbor interaction, in combination with the crystallographic superstructure, which involves small displacements of the nickel atoms in between next-nearest uranium atoms. Our magnetization model, based upon the decomposition of the spin system into two separate subsystems, has provided us the magnetic phase diagram and the field-induced spin structures. These involve small rotations of the magnetic moments, which only slowly align with the external field. Our model qualitatively reproduces the experimental phase diagram, but the in-field spin structures should be established by direct techniques.

We have analyzed the behavior of $UNi_4B$ in zero and low magnetic fields in terms of unique magnetic ordering and one-dimensional ferromagnetic excitations in the chains of paramagnetic U spins. The excitations of these spins give rise to increasing susceptibility and electronic specific heat below $T_N$, and weak power-law behavior of specific heat and resistivity. Here we have demonstrated that the application of large magnetic fields in the basal-plane direction quenches the influence of these excitations, giving way to the regular behavior of an antiferromagnet, albeit it with a complex ordered structure, with several spin-reorientation phases. We propose that the crossover line in the phase diagram is related to this quenching. At the highest fields, the paramagnetic spins attain the same moment value as the ordered spins. Further neutron-diffraction studies on single crystals in magnetic fields are underway to establish the nature of the spin-reorientation phases and possible unusual critical behavior, as expected for ordering on triangular lattices with antiferromagnetic interactions.

## ACKNOWLEDGMENTS

We acknowledge C.E. Snel, T.J. Gortenmulder, and R.W.A. Hendrikx for their ongoing technical support. Part of this research was supported by the Stichting voor Fundamenteel Onderzoek der Materie (FOM), which is financially supported by the Nederlandse Organisatie voor Wetenschappelijk Onderzoek (NWO).

* Present address: Department of Physics, University of Toronto, 60 St. George St., Toronto, Ontario, Canada M5S 1A7.

† Present address: LANSCE, Los Alamos National Laboratories, MS H805, Los Alamos, NM 87545.

[1] S.A.M. Mentink, A. Drost, G.J. Nieuwenhuys, E. Frikkee, A.A. Menovsky, and J.A. Mydosh, Phys. Rev. Lett. **73**, 1031 (1994).

[2] S.A.M. Mentink, H. Nakotte, A. de Visser, A.A. Menovsky, G.J. Nieuwenhuys, and J.A. Mydosh, Physica B **186-188**, 270 (1993).

[3] S.A.M. Mentink, G.J. Nieuwenhuys, A.A. Menovsky, and J.A. Mydosh, Physica B **194-196**, 275 (1994).

[4] A. Drost, Ph.D. thesis, Leiden University, 1995 (unpublished).

[5] See, e.g., S.C. Miller and W.F. Love, *Representations of Space Groups and Co-representations of Magnetic Space Groups* (Pruett Press, Boulder, CO, 1967).

[6] M.W. Meisel *et al.* (unpublished).

[7] G.J. Nieuwenhuys *et al.*, in Proceedings of the International Conference on Strongly Correlated Electron Systems 1994 [Physica B (to be published)].

[8] S.A.M. Mentink, G.J. Nieuwenhuys, A.A. Menovsky, J.A. Mydosh, K. Sugiyama, Y. Bando, and T. Takabatake, in Proceedings of the International Conference on Magnetism 1994 [Physica B (to be published)].
[9] F. Boersma, W.J.M. de Jonge, and K. Kopinga, Phys. Rev. B **23**, 186 (1981).
[10] J. Villain and J.M. Loveluck, J. Phys. (Paris) Lett. **38**, L77 (1977).
[11] D.J. Scalapino, Y. Imry, and P. Pincus, Phys. Rev. B **11**, 2042 (1975).
[12] J.C. Bonner and M.E. Fisher, Phys. Rev. A **135**, 640 (1964).
[13] S.A.M. Mentink, G.J. Nieuwenhuys, A.A. Menovsky, J.A. Mydosh, A. Drost, and E. Frikkee, in Proceedings of the International Conference on Strongly Correlated Electron Systems 1994 [Physica B (to be published)].
[14] M.L. Plumer, A. Mailhot, and A. Caillé, Phys. Rev. B **48**, 34840 (1993); **49**, 15133 (1994).